Free-Radical Polymerization of Styrene with a Binary Mixture of Symmetrical Bifunctional Initiators

WON JUNG YOON and KYU YONG CHOI*

Department of Chemical Engineering, University of Maryland, College Park, Maryland 20742

SYNOPSIS

The kinetics of bulk styrene polymerization catalyzed by a binary mixture of symmetrical bifunctional initiators has been investigated. When the bifunctional initiators having different thermal stabilities are mixed, an unsymmetry in the initiator functions is formed *in situ* via propagation, chain transfer, and termination reactions. For the quantification of the polymerization kinetics, a kinetic model has been developed using the molecular species modeling technique. For various polymerization conditions, good agreements between the model predictions and experimental data have been obtained. It is shown that polymerization rate and molecular weight can be easily regulated under isothermal reaction condition by changing the initiator composition. A comparison of the detailed kinetic model with a simple kinetic model for monofunctional initiators has also been made to illustrate the molecular weight increasing effect of the bifunctional initiator system. © 1992 John Wiley & Sons, Inc.

INTRODUCTION

Bifunctional initiators containing two labile groups of equal or unequal thermal stabilities are frequently used in the polymer industry for the synthesis of vinyl polymers. In our previous reports, we have presented the kinetic models for styrene polymerization with a single symmetrical bifunctional initiator and with a single unsymmetrical bifunctional initiator.[1-5] Although these models were developed for styrene polymerization, they can be used for other vinyl monomer polymerizations with minor modifications. One of the potential advantages of using bifunctional initiators, in particular unsymmetrical ones, in free-radical polymerization is that high polymerization rate and high polymer molecular weight can be readily obtained simultaneously by employing appropriate reactor temperature programming. In other words, one can have a better control of radical concentration even at high reaction temperature without undesired initiator burnouts (e.g., dead-end polymerization). Another advantage of using unsymmetrical bifunctional initiator is that little or no modification of reactor equipment is required to use them in the existing polymerization facility. For example, when unsymmetrical bifunctional initiators are used in suspension polymerization, controlled initiation can be easily obtained without adding the second initiator to the reactor where the efficient initiator migration from the aqueous phase to viscous or hardening polymer particles is difficult to achieve.

Since there are a few symmetrical bifunctional initiators available in commercial quantity, it is of practical interest to form *in situ* unsymmetry of initiator functions by mixing more than one symmetrical bifunctional initiators of different thermal stabilities. Quite obviously, one can expect that the resulting reaction kinetics will be quite complicated because there are repeated reinitiation, propagation, chain transfer, and chain termination reactions due to the presence of undecomposed labile groups residing in the polymer chain ends. Here, we need a model that can provide an accurate prediction of polymerization rate and resulting polymer molecular weight properties. In this paper, we shall present a kinetic model for free-radical styrene polymerization with a binary mixture of symmetrical bifunctional

* To whom correspondence should be addressed.

Journal of Applied Polymer Science, Vol. 46, 1353–1367 (1992)
 CCC 0021-8995/92/081353-15

initiators. Polymerization experiments have also been carried out under various reaction conditions in order to validate the proposed kinetic model.

REACTION KINETICS

The symmetrical bifunctional initiators to be considered in this study have two peroxide groups of equal thermal stability and they are represented by the following general form:

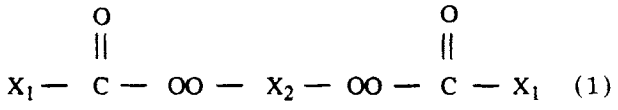

$$X_1-\overset{\overset{O}{\|}}{C}-OO-X_2-OO-\overset{\overset{O}{\|}}{C}-X_1 \quad (1)$$

where X_1 and X_2 are hydrocarbon ligands. The specific bifunctional initiators of the above structure used in our experimental study are 2,5-dimethyl-2,5-bis(benzoyl peroxy)hexane [Luperox 118; Initiator I_A] and 2,5-dimethyl-2,5-bis(2-ethyl hexanoyl peroxy)hexane [Lupersol 256; Initiator I_B]:

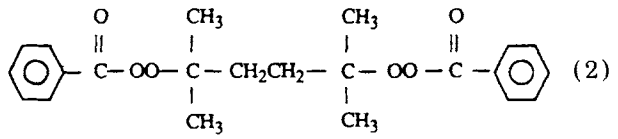

(2)

I_A

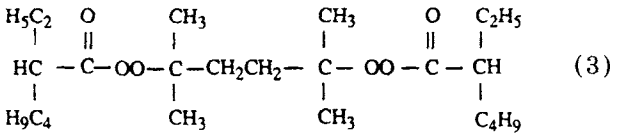

(3)

I_B

Since the peroxide groups in each initiator are separated by a fairly long hydrocarbon bridge for an inductive effect being negligible, the thermal stabilities of the peroxides are assumed not affected by whether or not the neighboring peroxide group has decomposed. Also notice that the hydrocarbon ligands between the two peroxide groups in both initiators are identical. The peroxide group in Luperox 118 has a half-life of 9.9 h at 100°C, whereas the peroxide group in Lupersol 256 has a half-life of 21 min at 100°C. Thus, Luperox 118 is a relatively *slow* bifunctional initiator and Lupersol 256 is a *fast* initiator. Primary radicals are generated by homolytic scission reactions as follows:

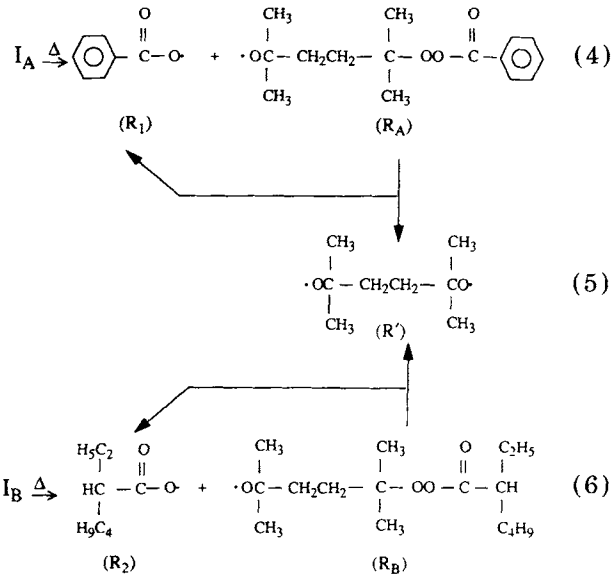

(4)

(5)

(6)

Note that when the primary radicals R_A and R_B decompose further, diradical species R' is generated. The primary radicals R_1 and R_2 may also undergo decarboxylation reactions, but there will be no net change in radical concentrations.

When styrene is polymerized by these radicals, undecomposed peroxides will be redistributed in the polymers via propagation, chain transfer, and termination reactions. Thus, for the quantification of the polymerization kinetics, we need to develop a kinetic model capable of predicting the polymerization rate and resulting polymer molecular weight. For the modeling of the polymerization kinetics, we shall use a molecular species modeling approach wherein polymer molecules are identified by the type of their end units. Table I shows 10 polymeric species present in the reaction mixture. The formation of these species is due to the presence of two different peroxide groups that are redistributed in the polymer chains through chain transfer and termination reactions. Note that there are two polymeric radical species (Q_n and S_n) containing an undecomposed peroxide and five inactive polymer species containing either one or two undecomposed peroxides (U_n, V_n, W_n, U'_n, and V'_n). Table II shows various reactions occurring in the reactor. We assume that the thermal stability of the peroxide in the polymer chains is independent of the polymer chain length and that the combination termination rate constants for the macroradical species are identical. Here, we also assume that no combination reactions occur between the primary radicals and that cyclization reaction is absent. The kinetic scheme shown in Table I is very similar to that with a single unsym-

Table I Polymeric Species

	Symbols	Note
P_n:	[———●	Live polymer without peroxides
Q_n:	A———●	Live polymer with undecomposed peroxide A
S_n:	B———●	Live polymer with undecomposed peroxide B
T_n:	●———●	Polymeric diradical
M'_n:	[———]	Dead polymer
U_n:	[———A	Inactive polymer with undecomposed peroxide A
V_n:	[———B	Inactive polymer with undecomposed peroxide B
W_n:	A———B	Inactive polymer with undecomposed peroxides A and B
U'_n:	A———A	Inactive polymer with two undecomposed peroxides A
V'_n:	B———B	Inactive polymer with two undecomposed peroxides B

metrical bifunctional initiator, implying that *in situ* initiator unsymmetry is readily obtained by mixing the two symmetrical bifunctional initiators.

With the kinetic scheme shown in Table II, we can write the rate equations for each species present in the reaction mixture as follows:

For Initiator and Primary Radicals:

$$\frac{1}{v}\frac{d}{dt}(I_A v) = -2k_{d_A} I_A \tag{7}$$

$$\frac{1}{v}\frac{d}{dt}(I_B v) = -2k_{d_B} I_B \tag{8}$$

$$\frac{1}{v}\frac{d}{dt}(R_A v) = 2f_A k_{d_A} I_A - k_{d_A} R_A - k_i R_A M \tag{9}$$

$$\frac{1}{v}\frac{d}{dt}(R_B v) = 2f_B k_{d_B} I_B - k_{d_B} R_B - k_i R_B M \tag{10}$$

$$\frac{1}{v}\frac{d}{dt}(Rv) = f_R[2k_{d_A} I_A + 2k_{d_B} I_B + k_{d_A} R_A + k_{d_B} R_B + k_{d_A}(Q + U + V + 2U') + k_{d_B}(S + V + W + 2V')] - k_i R M \tag{11}$$

$$\frac{1}{v}\frac{d}{dt}(R'v) = f_{R'}(k_{d_A} R_A + k_{d_B} R_B) - 2k_i R' M \tag{12}$$

Table II A Kinetic Model with a Binary Mixture of Symmetrical Bifunctional Initiators

Decomposition of peroxides

$I_A \xrightarrow{2k_{d_A}} R_1 + R_A$

$I_B \xrightarrow{2k_{d_B}} R_2 + R_B$

$R_A \xrightarrow{k_{d_A}} R_1 + R'$

$R_B \xrightarrow{k_{d_B}} R_2 + R'$

$Q_n \xrightarrow{k_{d_A}} R_1 + T_n \ (n \geq 1)$

$S_n \xrightarrow{k_{d_B}} R_2 + T_n \ (n \geq 1)$

$U_n \xrightarrow{k_{d_A}} R_1 + P_n \ (n \geq 2)$

$V_n \xrightarrow{k_{d_B}} R_2 + P_n \ (n \geq 2)$

$W_n \xrightarrow{k_{d_B}} R_2 + Q_n \ (n \geq 2)$

$W_n \xrightarrow{k_{d_A}} R_1 + S_n \ (n \geq 2)$

$U'_n \xrightarrow{2k_{d_A}} R_1 + Q_n \ (n \geq 2)$

$V'_n \xrightarrow{2k_{d_B}} R_2 + S_n \ (n \geq 2)$

Initiation

$R_1 + M \xrightarrow{k_i} P_1$

$R_2 + M \xrightarrow{k_i} P_1$

$R_A + M \xrightarrow{k_i} Q_1$

$R_B + M \xrightarrow{k_i} S_1$

$R' + M \xrightarrow[k_{dm}]{2k_i} T_1$

$3M \rightarrow 2P_1$ (*thermal initiation*)

Propagation ($n \geq 1$)

$P_n + M \xrightarrow{k_p} P_{n+1}$

$Q_n + M \xrightarrow{k_p} Q_{n+1}$

$S_n + M \xrightarrow{k_p} S_{n+1}$

$T_n + M \xrightarrow{2k_p} T_{n+1}$

Chain transfer ($n \geq 1$)

$P_n + M \xrightarrow{k_{fm}} M_n + P_1$

$Q_n + M \xrightarrow{k_{fm}} U_n + P_1$

$S_n + M \xrightarrow{k_{fm}} V_n + P_1$

$T_n + M \xrightarrow{2k_{fm}} P_n + P_1$

Termination ($n, m \geq 1$)

$P_n + P_m \xrightarrow{k_t} M'_{n+m}$

$P_n + Q_m \xrightarrow{k_t} U_{n+m}$

$P_n + S_m \xrightarrow{k_t} V_{n+m}$

$P_n + T_m \xrightarrow{2k_t} P_{n+m}$

$Q_n + Q_m \xrightarrow{k_t} U'_{n+m}$

$Q_n + S_m \xrightarrow{k_t} W_{n+m}$

$Q_n + T_m \xrightarrow{2k_t} Q_{n+m}$

$S_n + S_m \xrightarrow{k_t} V'_{n+m}$

$S_n + T_m \xrightarrow{2k_t} S_{n+m}$

$T_n + T_m \xrightarrow{4k_t} T_{n+m}$

Table III Numerical Values of Kinetic Parameters

	Ref.
$k_{d_A} = 4.267 \times 10^{18}\exp(-36{,}800/RT)$, min^{-1}	6
$k_{d_B} = 1.251 \times 10^{17}\exp(-31{,}700/RT)$, min^{-1}	6
$k_{dm} = 1.314 \times 10^{7}\exp(-27{,}440/RT)$, min^{-1}	7
$k_p = 6.306 \times 10^{8}\exp(-7{,}060/RT)$, L/mol min	8
$k_{t0} = 7.530 \times 10^{10}\exp(-1{,}680/RT)$, L/mol min	8
$k_i \approx k_p$	
$k_{f0} = 2.319 \times 10^{8}\exp(-10{,}790/RT)$, L/mol min	5
$M_0 = 8.728$ mol/L	
$\epsilon = -0.147$	9
$g_t \equiv \frac{k_t}{k_{t0}} \equiv \frac{k_{fm}}{k_{f0}} = \exp[-2(Bx + Cx^2 + Dx^3)]$	3, 10
$B = 2.5882 - 3.4852 \times 10^{-3}\ T\ (K)$	
$C = 4.3108 - 1.2635 \times 10^{-2}\ T\ (K)$	
$D = -4.6488 + 1.9026 \times 10^{-2}\ T\ (K)$	

For Growing Polymers:

$$\frac{1}{v}\frac{d}{dt}(P_1 v) = 2k_{dm}M^3 + k_i RM + k_{d_A}U_1 + k_{d_B}V_1 - k_p MP_1 + k_{fm}(P - P_1 + Q + S + 2T + 2T_1) - k_t P_1(P + Q + S + 2T) \quad (13)$$

$$\frac{1}{v}\frac{d}{dt}(P_n v) = k_{d_A}U_n + k_{d_B}V_n + k_p M(P_{n-1} - P_n) + k_{fm}M(2T_n - P_n) - k_t P_n(P + Q + S + 2T) + 2k_t \sum_{m=1}^{n-1} P_{n-m}T_m \quad (n \geq 2) \quad (14)$$

$$\frac{1}{v}\frac{d}{dt}(Q_1 v) = k_i R_A M - k_{d_A}Q_1 - k_p MQ_1 - k_{fm}MQ_1 - k_t Q_1(P + Q + S + 2T) \quad (15)$$

$$\frac{1}{v}\frac{d}{dt}(Q_n v) = k_{d_A}Q_n + k_{d_B}W_n + 2k_{d_A}U'_n + k_p M(Q_{n-1} - Q_n) - k_{fm}MQ_n - k_t Q_n(P + Q + S + 2T) + 2k_t \sum_{m=1}^{n-1} Q_{n-m}T_m \quad (n \geq 2) \quad (16)$$

$$\frac{1}{v}\frac{d}{dt}(S_1 v) = k_i R_B M - k_{d_B}S_1 - k_p MS_1 - k_{fm}MS_1 - k_t S_1(P + Q + S + 2T) \quad (17)$$

$$\frac{1}{v}\frac{d}{dt}(S_n v) = -k_{d_B}S_n + k_{d_A}W_n + 2k_{d_B}V'_n + k_p M(S_{n-1} - S_n) - k_{fm}MS_n - k_t S_n(P + Q + S + 2T) + 2k_t \sum_{m=1}^{n-1} S_{n-m}T_m \quad (n \geq 2) \quad (18)$$

$$\frac{1}{v}\frac{d}{dt}(T_1 v) = 2k_i R'M + k_{d_A}Q_1 + k_{d_B}S_1 - 2k_p MT_1 - 2k_{fm}MT_1 - 2k_t T_1(P + Q + S + 2T) \quad (19)$$

$$\frac{1}{v}\frac{d}{dt}(T_n v) = k_{d_A}Q_n + k_{d_B}S_n + 2k_p M(T_{n-1} - T_n) - 2k_{fm}MT_n - 2k_t T_n(P + Q + S + 2T) + 2k_t \sum_{m=1}^{n-1} T_{n-m}T_m \quad (n \geq 2) \quad (20)$$

For Temporarily Inactive Polymers:

$$\frac{1}{v}\frac{d}{dt}(U_1 v) = -k_{d_A}U_1 + k_{fm}MQ_1 \quad (21)$$

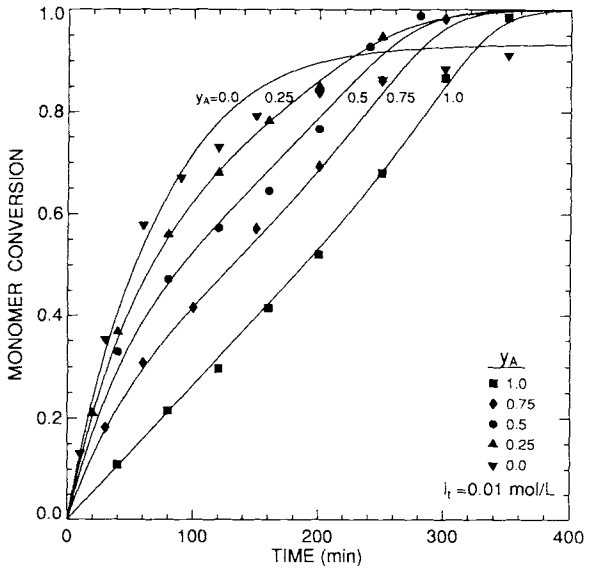

Figure 1 Effect of initiator mixture composition on monomer conversion (I_t = 0.01 mol/L, 100°C).

$$\frac{1}{v}\frac{d}{dt}(U_n v) = -k_{d_A}U_n + k_{fm}M\dot{Q}_n + k_t\sum_{m=1}^{n-1}P_{n-m}Q_m \quad (n \geq 2) \quad (22)$$

$$\frac{1}{v}\frac{d}{dt}(V_1 v) = -k_{d_B}V_1 + k_{fm}MS_1 \quad (23)$$

$$\frac{1}{v}\frac{d}{dt}(V_n v) = -k_{d_B}V_n + k_{fm}MS_n + k_t\sum_{m=1}^{n-1}P_{n-m}S_m \quad (n \geq 2) \quad (24)$$

$$\frac{1}{v}\frac{d}{dt}(W_n v) = -(k_{d_A} + k_{d_B})W_n + k_t\sum_{m=1}^{n-1}Q_{n-m}S_m \quad (n \geq 2) \quad (25)$$

$$\frac{1}{v}\frac{d}{dt}(U'_n v) = -2k_{d_A}U'_n + \frac{1}{2}k_t\sum_{m=1}^{n-1}Q_{n-m}Q_m \quad (n \geq 2) \quad (26)$$

$$\frac{1}{v}\frac{d}{dt}(V'_n v) = -2k_{d_B}V'_n + \frac{1}{2}k_t\sum_{m=1}^{n-1}S_{n-m}S_m \quad (n \geq 2) \quad (27)$$

For Monomers and Dead Polymers:

$$\frac{1}{v}\frac{d}{dt}(Mv) = -3k_{dm}M^2 - k_i(R + R_A + R_B + 2R')M - k_{fm}M(P + Q + S + 2T) - k_pM(P + Q + S + 2T) \quad (28)$$

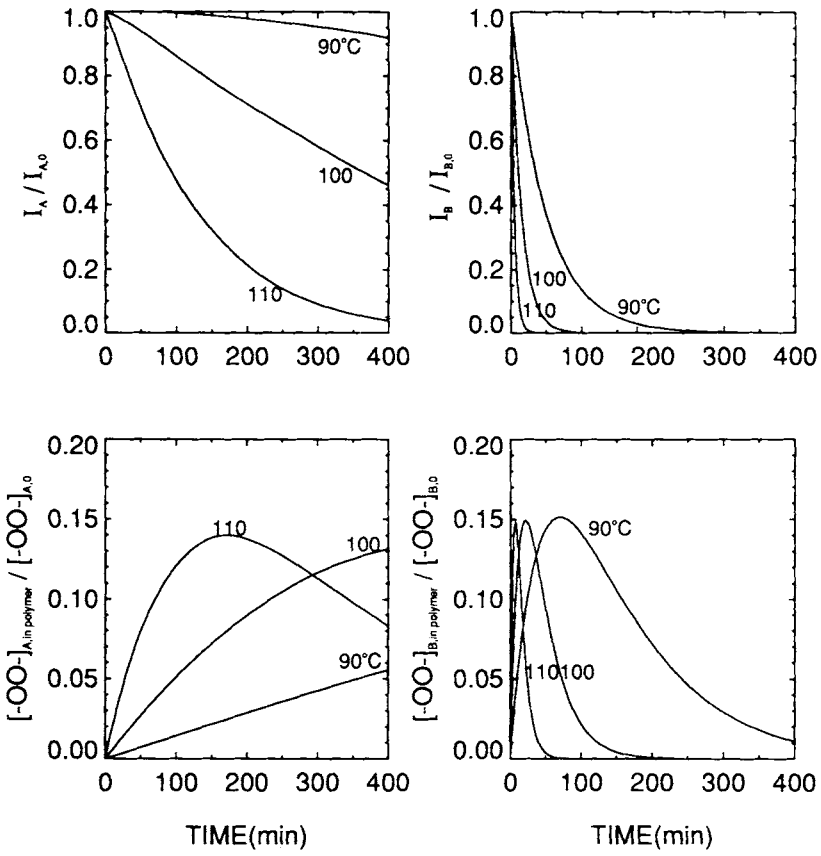

Figure 2 Concentration profiles of initiators and undecomposed peroxides in polymers (I_t = 0.01 mol/L, y_A = 0.5) [model simulation].

$$\frac{1}{v}\frac{d}{dt}(M'_n v) = k_{fm} M P_n + \frac{1}{2} k_t \sum_{m=1}^{n-1} P_{n-m} P_m \quad (n \geq 2) \quad (29)$$

where P, Q, S, T, U, V, W, U', and V' are the total concentrations of the corresponding polymeric species, i.e.,

$$P = \sum_{n=1}^{\infty} P_n, \quad Q = \sum_{n=1}^{\infty} Q_n, \quad S = \sum_{n=1}^{\infty} S_n,$$

$$T = \sum_{n=1}^{\infty} T_n, \quad U = \sum_{n=1}^{\infty} U_n, \quad V = \sum_{n=1}^{\infty} V_n,$$

$$W = \sum_{n=2}^{\infty} W_n, \quad U' = \sum_{n=2}^{\infty} U'_n, \quad V' = \sum_{n=2}^{\infty} V'_n \quad (30)$$

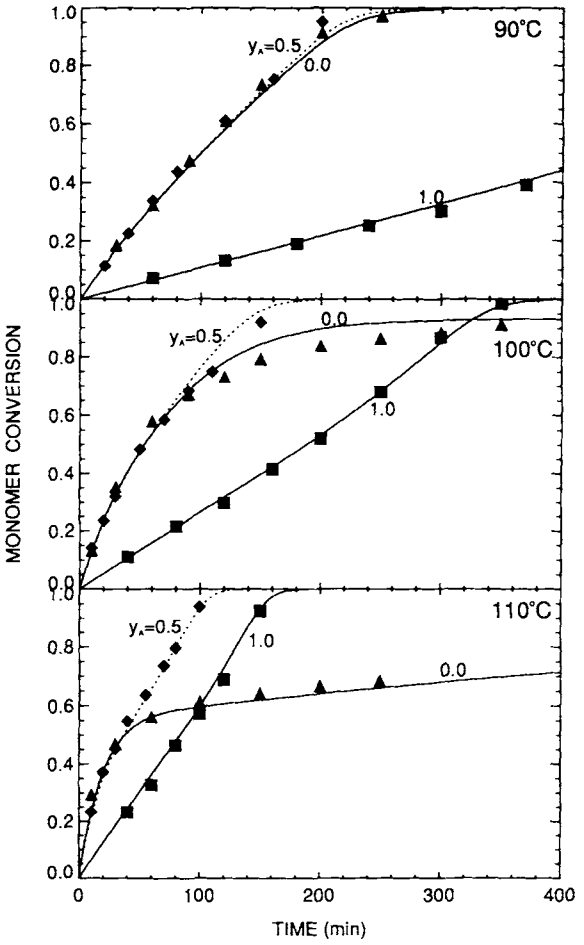

Figure 3 Monomer conversion profiles for initiator mixture and single initiators: (♦) I_t = 0.02 mol/L, y_A = 0.5; (■) [Luperox 118] = 0.01 mol/L; (▲) [Lupersol 256] = 0.01 mol/L.

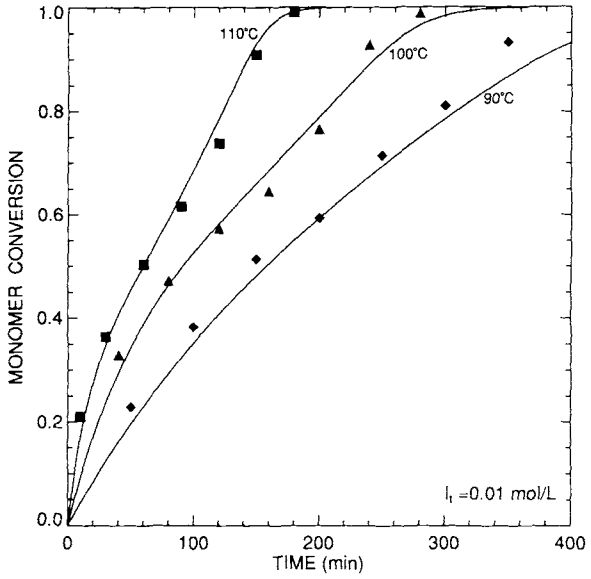

Figure 4 Effect of polymerization temperature (I_t = 0.01 mol/L, y_A = 0.5).

In the above equations, v is the volume of the reaction mixture. The volume change is described by

$$\frac{1}{v}\frac{d}{dt} = -\frac{\epsilon}{M_0 + \epsilon M}\frac{dM}{dt} \quad (31)$$

where M_0 is the initial monomer concentration, and ϵ, the volume contraction factor. The gel effect correlation used in our previous works is used here to account for the diffusion-controlled termination reactions at high monomer conversion. In the above kinetic model, $R = R_1 + R_2$ and it is assumed that the reactivities of R_1 and R_2 are same.

In describing the polymerization kinetics, we should consider some loss of primary radicals due to side reactions. Thus, the initiator efficiency factor is used to account for the loss of primary radicals that are not used for chain initiation reactions. In our previous works,[4,5] it was observed that the initiator efficiency factor was a linear function of peroxide group concentrations. We used the following empirical correlation obtained in Ref. 5 to estimate the initiator efficiency factor:

$$f_i = 0.633 - 4.929[\text{—}OO\text{—}]_0 \quad (32)$$

where $[\text{—}OO\text{—}]_0$ is the initial peroxide group concentration in the reactor. We assumed that each peroxide group has identical initiation efficiency and that the efficiency is constant throughout the po-

lymerization process. The numerical values of various kinetic parameters used in our model simulations are listed in Table III. The molecular weight moment equations used to calculate the polymer molecular weight averages are shown in the Appendix. These moment equations are solved simultaneously with the kinetic modeling equations shown above by using the fourth-order Runge–Kutta method.

EXPERIMENTAL

Polymerization experiments were carried out using Pyrex ampules (o.d. 5 mm). Styrene (Aldrich) was passed through an Amberlyst-27 column (Rohm and Haas) to remove inhibitors. The bifunctional initiators (Luperox 118 and Lupersol 256, ATOCHEM) were used as supplied. Each ampule containing the monomer and initiator mixture was purged with nitrogen and degassed by many successive freeze-thaw cycles in acetone and a dry-ice mixture until no bubbles could be seen. When the bath temperature reached the desired reaction temperature, all the ampules were dipped into the bath. After the polymerization, the polymer samples were dissolved in toluene and precipitated by adding excess methanol. This procedure was repeated several times to ensure that unreacted monomer was completely

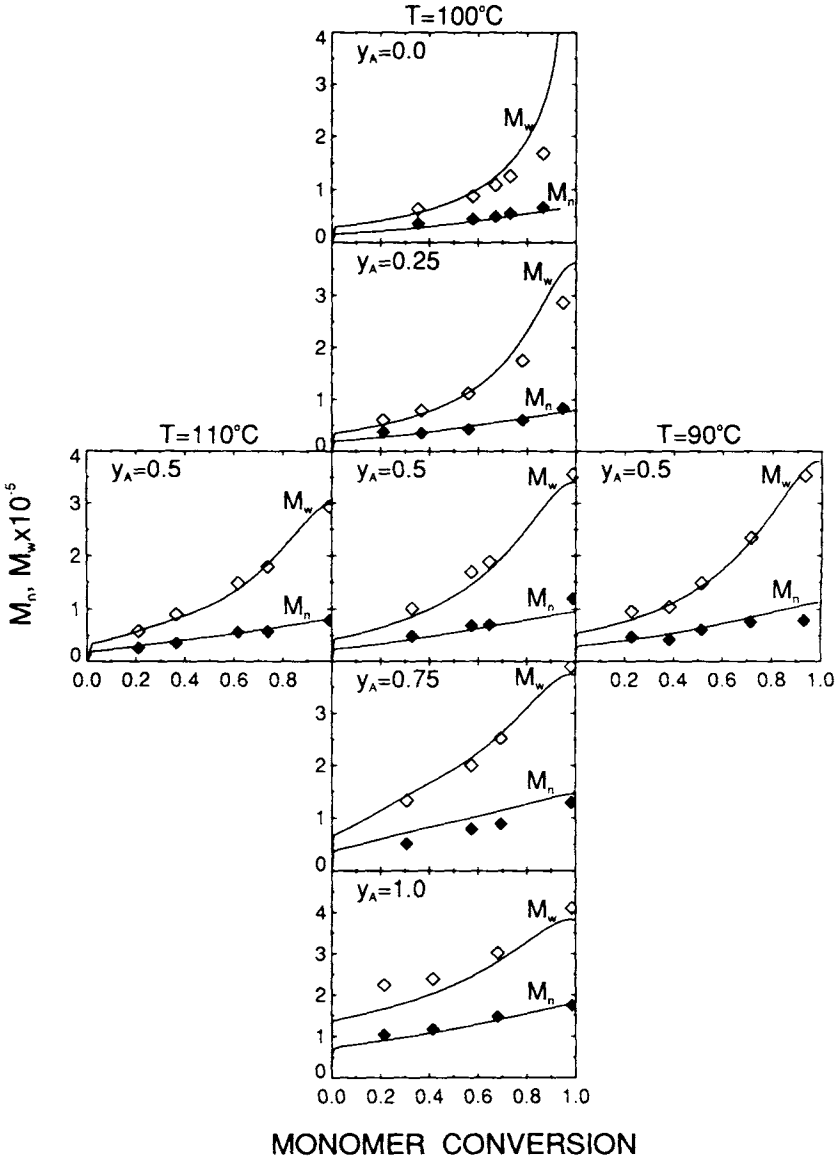

Figure 5 Effect of temperature and initiator composition on polymer molecular weight.

removed from the polymer. The samples were dried *in vacuo*, and the monomer conversion was measured by the gravimetric method. Some experiments were duplicated and excellent reproducibility was obtained. To confirm the isothermal reaction conditions, several test experiments were conducted by inserting a thermocouple into the ampule and monitoring the reaction temperature. For the reaction temperatures and initiator concentrations employed in this work, the maximum temperature difference between the oil bath and the reaction mixture was less than 1°C. The polymer molecular weight and molecular weight distribution were determined by gel permeation chromatography with four Ultrastyragel columns (Waters: 10^4, 10^3, 500 Å, and linear) and tetrahydrofuran as a solvent.

RESULTS AND DISCUSSION

When the two symmetrical bifunctional initiators are mixed, the initiator mixture composition is a new free parameter one can use to regulate the polymerization rate. With the total initiator concentration fixed at 0.01 mol/L, the polymerization experiments were carried out at 100°C for five different initiator compositions. Figure 1 shows the monomer conversion profiles where y_A is the mol fraction of Luperox 118 (*slow initiator*). Here, solid lines represent the model simulations. As shown, excellent agreements between the model predictions and the experimental data have been obtained for all the cases studied. It is seen that when pure Lupersol 256 is used (i.e., $y_A = 0.0$) at 100°C, dead-end polymerization occurs, limiting the final monomer conversion to 90%. When the slow initiator (Luperox 118) is used alone (i.e., $y_A = 1.0$), higher monomer conversion is obtained, but a quite longer reaction time is required. As Luperox 118 is added to Lupersol 256, the polymerization rate decreases to some extent, but no dead-end polymerization occurs and higher monomer conversion is obtained in less reaction time than with Luperox 118 alone. The reason for the disappearance of dead-end polymerization is that after the depletion of less stable peroxide B in Lupersol 256 there is a continuing supply of radicals by the slowly decomposing Luperox 118.

In Figure 1, we can observe a break in the monomer conversion curve for $y_A = 0.25$, 0.5, and 0.75, indicating that as the peroxide group B in Lupersol 256 is depleted the other peroxide A in Luperox 118 decomposes further to drive the reaction to higher conversion. A similar phenomenon has also been observed in the styrene polymerization initiated by unsymmetrical bifunctional initiators[4] and polyfunctional initiators.[11,12] In general, the greater the dissimilarity in the thermal stabilities of the peroxide groups, the more pronounced is the break on the monomer conversion curves. Figure 2 shows the concentration profiles of peroxide groups A and B in the primary initiators and in the polymers. Notice that even after the complete decomposition of primary initiator B some peroxide groups are still present in the polymers.

The effect of initiator composition is more clearly seen in Figure 3 where a 50/50 (mol ratio) mixture of the symmetrical bifunctional initiators is used at fixed total initiator concentration (0.02 mol/L). Also shown are the monomer conversion profiles with a single symmetrical bifunctional initiator. At 90°C, the monomer conversion with the mixture is almost the same as that with pure Lupersol 256, because at this temperature, Luperox 118 (slow initiator) decomposes only a little. As the reaction temperature is increased (e.g., 110°C), the initiator mixture clearly shows its effect. For example, during the initial reaction period, the rate of polymerization is the same as that with Lupersol 256 alone, but after about 55% conversion, the overall polymerization rate becomes very close to that with pure Luperox 118. Thus, one can obtain the monomer conversion of 0.6–1.0 in much reduced reaction time by using a mixture of these symmetrical bifunctional initiators. Notice that with Lupersol 256 alone at

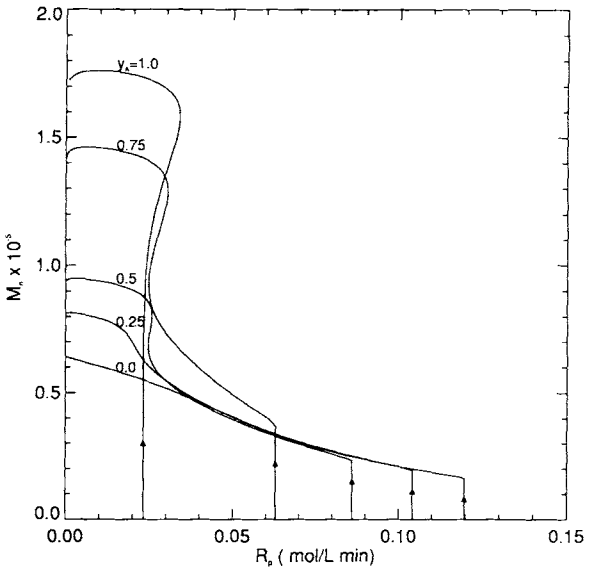

Figure 6 M_n vs. R_p curves (I_t = 0.01 mol/L, 100°C) [model simulation].

110°C the final monomer conversion is limited to only 65% because of the occurrence of dead-end polymerization.

The effect of reaction temperature was investigated by carrying out the polymerization experiments for $y_A = 0.5$ with the total initiator concentration of 0.01 mol/L at three different temperatures, i.e., 90, 100, and 110°C. Figure 4 shows that very high monomer conversion is obtainable by using the initiator mixture at high temperatures and that the agreement between the model predictions and experimental data is again very satisfactory. A break in the monomer conversion curve is also more pronounced at higher temperatures.

The number-average molecular weight (M_n) and the weight-average molecular weight (M_w) of polystyrene are shown in Figure 5 for different initiator compositions at different temperatures (for $y_A = 0.5$). As shown, the overall model predictions are very accurate. It should be noted that no bimodal molecular weight distribution was observed in all the polymer samples we analyzed. Figure 5 also indicates that the polydispersity (M_w/M_n) tends to increase at high monomer conversion with a mixed

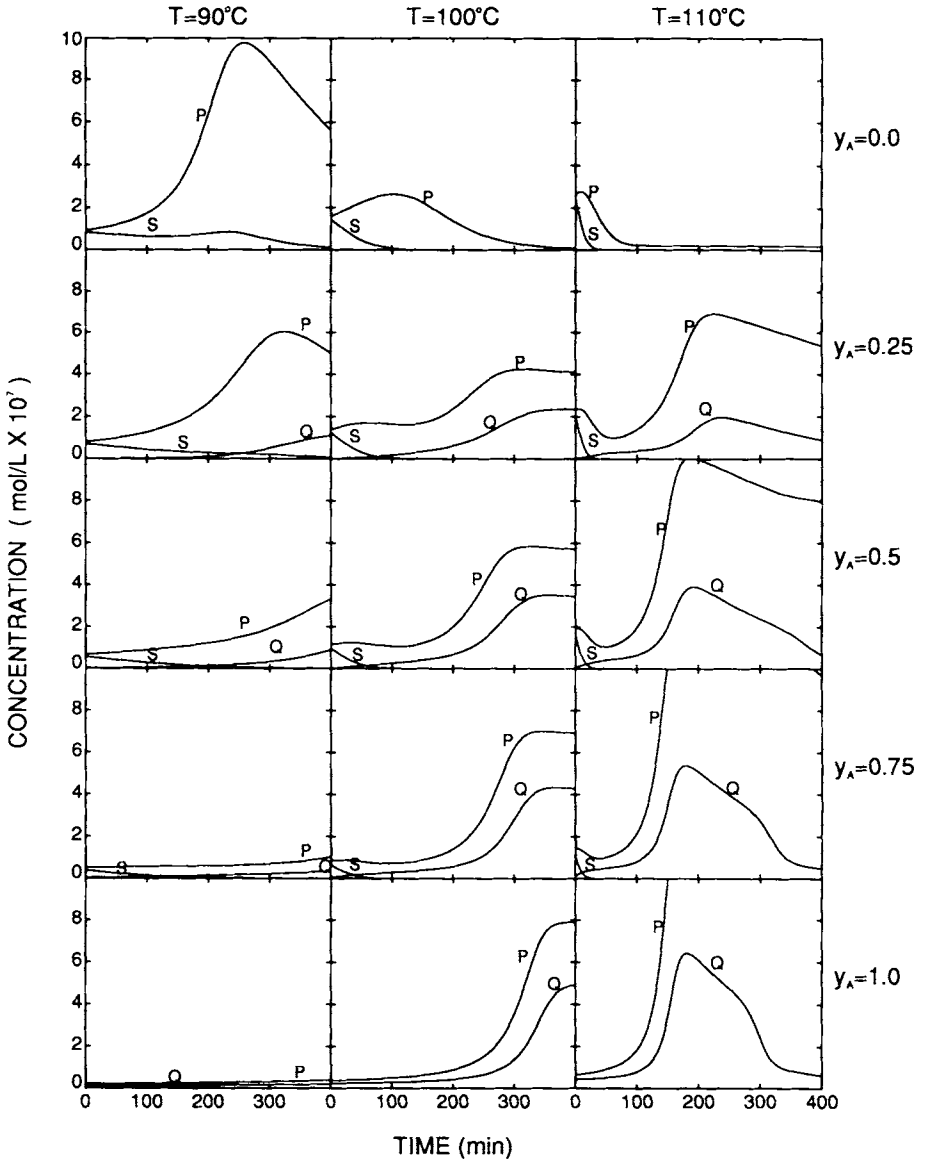

Figure 7 Effect of initiator composition and reaction temperature on live polymer concentrations [model simulation].

initiator system. Figure 6 shows M_n vs. R_p (polymerization rate) for five different initiator compositions at 100°C. The arrows in the curves indicate the direction of reaction progress in time. With Luperox 118 alone ($y_A = 1.0$), the polymerization rate is very low and almost constant until high conversion is reached but highest molecular weight is obtained. Contrarily, when Lupersol 256 is used alone ($y_A = 0.0$), the highest polymerization rate is obtained but the resulting polymer molecular weight is the lowest. When these initiators are mixed, the intermediate reaction rate and molecular weight are obtainable. This is important because now one can better optimize the polymerization process to obtain desired polymer molecular weight in reduced reaction time by simply changing the initiator composition even under isothermal reaction conditions.

The concentrations of live polymers during the course of polymerization are illustrated in Figure 7 for varying reaction temperatures and initiator compositions (Note: $P = \Sigma P_n$, $Q = \Sigma Q_n$, $S = \Sigma S_n$). The concentration of diradical species (T_n) is so low that it is not shown in the figure. It is seen that for a given initiator composition reaction temperature has a strong effect on the formation of various live polymers. It is interesting to observe that at 90°C the concentration of P_n species increases as y_A is decreased (i.e., more Lupersol 256), whereas at higher temperatures (e.g., 110°C), the concentration of P_n species decreases as y_A is decreased. The weight fraction and number-averages degree of polymerization at 90, 100, and 110°C for inactive polymer species are shown in Figure 8 with $y_A = 0.5$. At relatively low temperature (e.g., 90°C), the concentrations of inactive polymers capped by either A or B peroxide (i.e., U_n and V_n species) are both high; however, as the reaction temperature is increased, the peroxide B decomposes rapidly to result in much lower concentration of V_n species. V'_n polymers that contain two undecomposed B peroxides on both chain ends have the largest chain length. Among the five inactive polymers containing at least one undecomposed peroxide, W_n species has the lowest concentration.

In the foregoing discussion, we showed that the proposed kinetic model provides an adequate prediction of both polymerization rate and polymer molecular weight. At this point, it would be of interest to evaluate the need for the detailed kinetic model as proposed in this paper from a different angle. To do so, let us assume that we view the mixture of the symmetrical bifunctional initiators as simply a mixture of two types of peroxide A and B in *hypothetical* monofunctional initiators. Since the

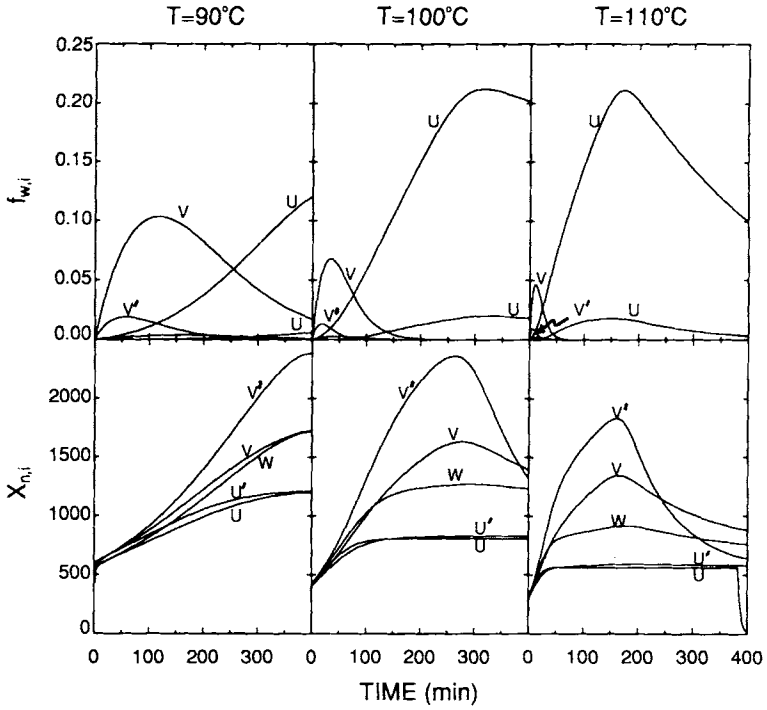

Figure 8 Weight fractions and number-average chain length of inactive polymeric species ($I_t = 0.01$ mol/L, $y_A = 0.5$) [model simulation].

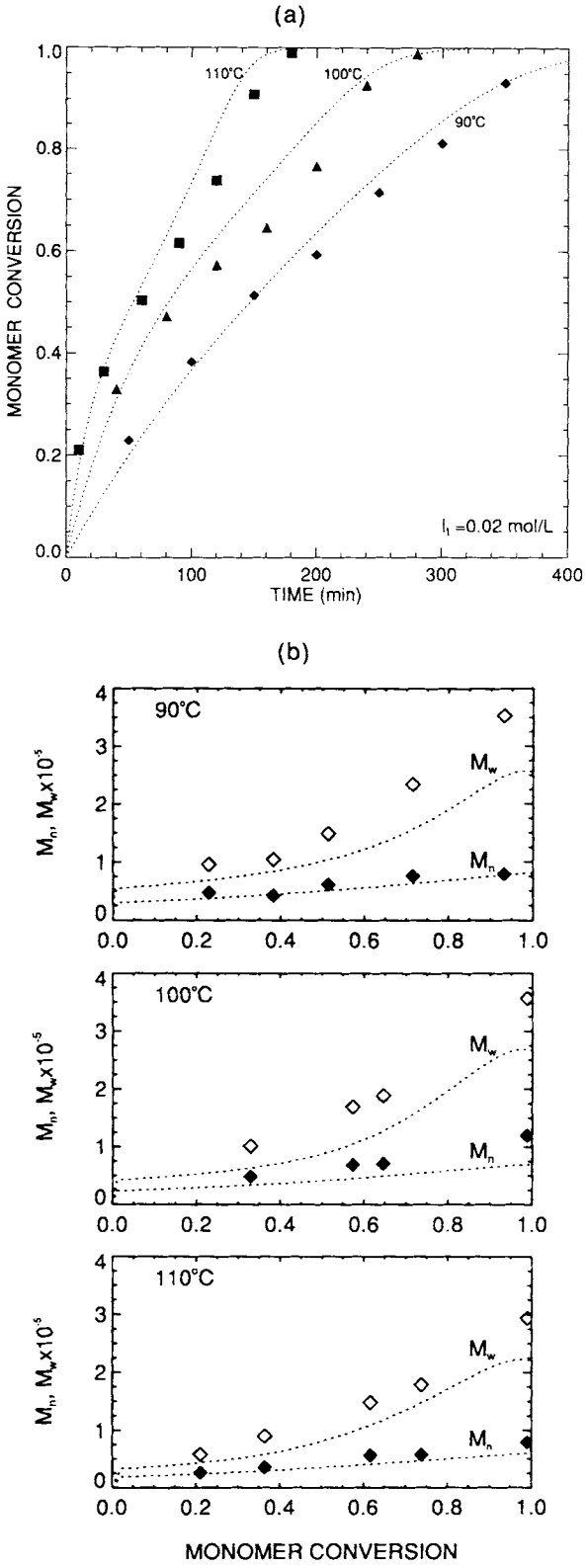

Figure 9 (a) Monomer conversion profiles predicted by a simple model (I_t = 0.02 mol/L). (b) Molecular weight profiles predicted by a simple model (I_t = 0.02 mol/L).

decomposition of these peroxides is solely due to thermal activation, we may expect that the monomer conversion or the polymerization rate could be predicted with a simple kinetic model.[2] Thus, we carried out the simulations of the kinetic model for a binary mixture of *hypothetical* monofunctional initiators. Figure 9(a) shows the predicted monomer conversion profiles at $[-OO-]_A$ = 0.01 mol/L and $[-OO-]_B$ = 0.01 mol/L at three different temperatures. Figure 9(b) shows the resulting polymer molecular weight predictions. The experimental data are for a 50/50 mixture of Luperox 118 and Lupersol 256. Although the monomer conversion predictions are not as good as shown in Figure 4, the overall accuracy of the simplified model is reasonably good. However, Figure 9(b) shows that the predicted molecular weight values, in particular M_w values, are significantly lower than the experimental values. Quite obviously, this is because in real polymerization systems there is an additional chain length extension mechanism due to the combination termination of growing polymer radicals containing undecomposed peroxide. When such peroxides in the polymer chains are decomposed and engaged in propagation and termination reactions, much larger polymer molecules are produced. Contrarily, no such chain-length extension mechanism is present in the mixture of the *hypothetical* monofunctional initiators. Thus, Figure 9(b) clearly illustrates the effect of *in situ* unsymmetry of the initiator functions on the increase in the polymer molecular weight as the mixture of symmetrical bifunctional initiators of different thermal stabilities is used in free-radical styrene polymerization.

CONCLUDING REMARKS

In this paper, we have presented a kinetic model for styrene polymerization with a binary mixture of symmetrical bifunctional initiators. The model was validated experimentally by using two commercially available symmetrical bifunctional initiators. An excellent agreement between the model predictions and the experimental data was obtained for all the cases studied. It was shown that polymerization rate and polymer molecular weight can be regulated by employing the appropriate initiator composition and reaction temperature. Even at fixed reaction temperature, one can obtain a broad range of molecular weight values by simply varying the initiator composition. It has also been shown that using a simple model for the mixture of monofunctional initiators

is not adequate in predicting the polymer molecular weight.

Acknowledgment is made to the Donors of the Petroleum Research Funds, administered by the American Chemical Society, for support of this research (20223-AC7). A partial support was also provided by the National Science Foundation (CBT-85-52428).

APPENDIX

A. Definition of Polymer Molecular Weights and Average Chain Length

Polymer Molecular Weight Moments

$$\lambda_{\xi,k} \equiv \sum_{n=j}^{\infty} n^k \xi_n \quad [\xi = P, Q, S, T, U, V (j = 1); W, U', V' (j = 2)] \quad \text{(A.1)}$$

$$\lambda_k^d \equiv \sum_{n=2}^{\infty} n^k M'_n \quad \text{(A.2)}$$

where $\lambda_{\xi,k}$ and λ_k^d denote the k-th moment of polymeric species ξ and dead polymers, respectively.

Number (X_n) and Weight (X_w) Average Chain Length

$$X_n = \frac{\sum_{\xi} \lambda_{\xi,1} + \lambda_1^d}{\sum_{\xi} \lambda_{\xi,0} + \lambda_0^d} \quad (\xi = P, Q, S, T, U, V, W, U', V') \quad \text{(A.3)}$$

$$X_w = \frac{\sum_{\xi} \lambda_{\xi,2} + \lambda_2^d}{\sum_{\xi} \lambda_{\xi,1} + \lambda_1^d} \quad (\xi = P, Q, S, T, U, V, W, U', V') \quad \text{(A.4)}$$

B. Molecular Weight Moment Equations

Polymeric Species, P_n

$$\frac{1}{v}\frac{d}{dt}(\lambda_{P,0} v)\left[= \frac{1}{v}\frac{d}{dt}(Pv)\right] = 2k_{dm}M^3 + k_i RM + k_{d_A} U + k_{d_B} V + k_{fm} M(Q + S + 4T) - k_t P(P + Q + S) \quad \text{(A.5)}$$

$$\frac{1}{v}\frac{d}{dt}(\lambda_{P,1} v) = 2k_{dm}M^3 + k_i RM + k_{d_A}\lambda_{U,1} + k_{d_B}\lambda_{V,1} + k_p MP + k_{fm} M(P - \lambda_{P,1} + Q + S + 2T + 2\lambda_{T,1}) + k_t[2P\lambda_{T,1} - (P + Q + S)\lambda_{P,1}] \quad \text{(A.6)}$$

$$\frac{1}{v}\frac{d}{dt}(\lambda_{P,2} v) = 2k_{d_m}M^3 + k_i RM + k_{d_A}\lambda_{U,2} + k_{d_B}\lambda_{V,2} + k_p M(2\lambda_{P,1} + P) + k_{fm} M(P - \lambda_{P,2} + Q + S + 2T + 2\lambda_{T,2}) + k_t[2P\lambda_{T,2} + 4k_t\lambda_{P,1}\lambda_{T,1} - (P + Q + S)\lambda_{P,2}] \quad \text{(A.7)}$$

Polymeric Species, Q_n

$$\frac{1}{v}\frac{d}{dt}(\lambda_{Q,0} v)\left[= \frac{1}{v}\frac{d}{dt}(Qv)\right] = k_i R_A M - k_{d_A} Q + k_{d_B} W + 2k_{d_A} U' - k_{fm} MQ - k_t Q(P + Q + S) \quad \text{(A.8)}$$

$$\frac{1}{v}\frac{d}{dt}(\lambda_{Q,1} v) = k_i R_A M - k_{d_A}\lambda_{Q,1} + k_{d_B}\lambda_{W,1} + 2k_{d_A}\lambda_{U',1} + k_p MQ - k_{fm} M\lambda_{Q,1} + k_t[2Q\lambda_{T,1} - (P + Q + S)\lambda_{Q,1}] \quad \text{(A.9)}$$

$$\frac{1}{v}\frac{d}{dt}(\lambda_{Q,2} v) = k_i R_A M - k_{d_A}\lambda_{Q,2} + k_{d_B}\lambda_{W,2} + 2k_{d_A}\lambda_{U',2} + k_p M(2\lambda_{Q,1} + Q) - k_{fm} M\lambda_{Q,2} + k_t[2Q\lambda_{T,2} + 4\lambda_{Q,1}\lambda_{T,1} - (P + Q + S)\lambda_{Q,2}] \quad \text{(A.10)}$$

Polymeric Species, S_n

$$\frac{1}{v}\frac{d}{dt}(\lambda_{S,0} v)\left[= \frac{1}{v}\frac{d}{dt}(Sv)\right] = k_i R_B M - k_{d_B} S + k_{d_A} W + 2k_{d_B} V' - k_{fm} MS - k_t S(P + Q + S) \quad \text{(A.11)}$$

$$\frac{1}{v}\frac{d}{dt}(\lambda_{S,1} v) = k_i R_B M - k_{d_B}\lambda_{S,1} + k_{d_A}\lambda_{W,1} + 2k_{d_B}\lambda_{V',1} + k_p MS - k_{fm} M\lambda_{S,1} + k_t[2S\lambda_{T,1} - (P + Q + S)\lambda_{S,1}] \quad \text{(A.12)}$$

$$\frac{1}{v}\frac{d}{dt}(\lambda_{S,2} v) = k_i R_B M - k_{d_B}\lambda_{S,2} + k_{d_A}\lambda_{W,2} + 2k_{d_B}\lambda_{V',2} + k_p M(2\lambda_{S,1} + S) - k_{fm} M\lambda_{S,2} + k_t[2S\lambda_{T,2} + 4\lambda_{S,1}\lambda_{T,1} - (P + Q + S)\lambda_{S,2}] \quad \text{(A.13)}$$

Polymeric Species, T_n

$$\frac{1}{v}\frac{d}{dt}(\lambda_{T,0}v)\left[=\frac{1}{v}\frac{d}{dt}(Tv)\right] = 2k_iR'M + k_{d_A}Q + k_{d_B}S - k_{fm}MT - 2k_t(P+Q+S+T)T \quad (A.14)$$

$$\frac{1}{v}\frac{d}{dt}(\lambda_{T,1}v) = 2k_iR'M + k_{d_A}\lambda_{Q,1} + k_{d_B}\lambda_{S,1} + 2k_pMT - k_{fm}M\lambda T, 1 - 2k_t(P+Q+S)\lambda_{T,1} \quad (A.15)$$

$$\frac{1}{v}\frac{d}{dt}(\lambda_{T,2}v) = 2k_iR'M + k_{d_A}\lambda_{Q,2} + k_{d_B}\lambda_{S,2} + 2k_pM(2\lambda_{T,1}+T) - k_{fm}M\lambda_{T,2} + 2k_t[2\lambda_{T,1}^2 - (P+Q+S)\lambda_{T,2}] \quad (A.16)$$

Polymeric Species, U_n

$$\frac{1}{v}\frac{d}{dt}(\lambda_{U,0}v)\left[=\frac{1}{v}\frac{d}{dt}(Uv)\right] = -k_{d_A}U + k_{fm}MQ + k_tPQ \quad (A.17)$$

$$\frac{1}{v}\frac{d}{dt}(\lambda_{U,1}v) = -k_{d_A}\lambda_{U,1} + k_{fm}M\lambda_{Q,1} + k_t(P\lambda_{Q,1} + \lambda_{P,1}Q) \quad (A.18)$$

$$\frac{1}{v}\frac{d}{dt}(\lambda_{U,2}v) = -k_{d_A}\lambda_{U,2} + k_{fm}M\lambda_{Q,2} + k_t(\lambda_{P,2}Q + 2\lambda_{P,1}\lambda_{Q,1} + P\lambda_{Q,2}) \quad (A.19)$$

Polymeric Species, V_n

$$\frac{1}{v}\frac{d}{dt}(\lambda_{V,0}v)\left[=\frac{1}{v}\frac{d}{dt}(Vv)\right] = -k_{d_B}V + k_{fm}MS + k_tPS \quad (A.20)$$

$$\frac{1}{v}\frac{d}{dt}(\lambda_{V,1}v) = -k_{d_B}\lambda_{V,1} + k_{fm}M\lambda_{S,1} + k_t(P\lambda_{S,1} + \lambda_{P,1}S) \quad (A.21)$$

$$\frac{1}{v}\frac{d}{dt}(\lambda_{V,2}v) = -k_{d_B}\lambda_{V,2} + k_{fm}M\lambda_{S,2} + k_t(\lambda_{P,2}S + 2\lambda_{P,1}\lambda_{S,1} + P\lambda_{S,2}) \quad (A.22)$$

Polymeric Species, W_n

$$\frac{1}{v}\frac{d}{dt}(\lambda_{W,0}v)\left[=\frac{1}{v}\frac{d}{dt}(Wv)\right] = -(k_{d_A}+k_{d_B})W + k_tQS \quad (A.23)$$

$$\frac{1}{v}\frac{d}{dt}(\lambda_{W,1}v) = -(k_{d_A}+k_{d_B})\lambda_{W,1} + k_t(\lambda_{Q,1}S + Q\lambda_{S,1}) \quad (A.24)$$

$$\frac{1}{v}\frac{d}{dt}(\lambda_{W,2}v) = -(k_{d_A}+k_{d_B})\lambda_{W,2} + k_t(\lambda_{Q,2}S + 2\lambda_{Q,1}\lambda_{S,1} + Q\lambda_{S,2}) \quad (A.25)$$

Polymeric Species, U'_n

$$\frac{1}{v}\frac{d}{dt}(\lambda_{U',0}v)\left[=\frac{1}{v}\frac{d}{dt}(U'v)\right] = -2k_{d_A}U' + \tfrac{1}{2}k_tQ^2 \quad (A.26)$$

$$\frac{1}{v}\frac{d}{dt}(\lambda_{U',1}v) = -2k_{d_A}\lambda_{U',1} + k_tQ\lambda_{Q,1} \quad (A.27)$$

$$\frac{1}{v}\frac{d}{dt}(\lambda_{U',2}v) = -2k_{d_A}\lambda_{U',2} + k_t(Q\lambda_{Q,2} + \lambda_{Q,1}^2) \quad (A.28)$$

Polymeric Species, V'_n

$$\frac{1}{v}\frac{d}{dt}(\lambda_{V',0}v)\left[=\frac{1}{v}\frac{d}{dt}(V'v)\right] = -2k_{d_B}V' + \tfrac{1}{2}k_tS^2 \quad (A.29)$$

$$\frac{1}{v}\frac{d}{dt}(\lambda_{V',1}v) = -2k_{d_B}\lambda_{V',1} + k_tS\lambda_{S,1} \quad (A.30)$$

$$\frac{1}{v}\frac{d}{dt}(\lambda_{V',2}v) = -2k_{d_B}\lambda_{V',2} + k_t(S\lambda_{S,2} + \lambda_{S,1}^2) \quad (A.31)$$

Polymeric Species, M'_n

$$\frac{1}{v}\frac{d}{dt}(\lambda_0^d v) = k_{fm}M(P - P_1) + \tfrac{1}{2}k_tP^2 \quad (A.32)$$

$$\frac{1}{v}\frac{d}{dt}(\lambda_1^d v) = k_{fm}M(\lambda_{P,1} - P_1) + k_tP\lambda_{P,1} \quad (A.33)$$

$$\frac{1}{v}\frac{d}{dt}(\lambda_2^d v) = k_{fm}M(\lambda_{P,2} - P_1) + k_t(P\lambda_{P,2} + \lambda_{P,1}^2) \quad (A.34)$$

C. Primary Radical Concentrations

$$R_A = \frac{2f_Ak_{d_A}I_A}{k_{d_A} + k_iM} \quad (A.35)$$

$$R_B = \frac{2f_Bk_{d_B}I_B}{k_{d_B} + k_iM} \quad (A.36)$$

$$R' = \frac{f_{R'}}{2k_iM}(k_{d_A}R_A + k_{d_B}R_B) \tag{A.37}$$

$$R = \frac{f_R}{k_iM}[2k_{d_A}I_A + 2k_{d_B}I_B + k_{d_A}(Q + U + W + 2U') + k_{d_B}(S + V + W + 2V') + k_{d_A}R_A + k_{d_B}R_B] \tag{A.38}$$

D. Concentrations of Primary Live Polymers

$$P_1 = \frac{2k_{dm}M^3 + k_iRM + k_{d_A}U_1 + k_{d_B}V_1}{(k_p + k_{fm})M + k_t(P + Q + S + 2T)} + \frac{k_{fm}M(P + Q + S + 2T + 2T_1)}{(k_p + k_{fm})M + k_t(P + Q + S + 2T)} \tag{A.39}$$

$$Q_1 = \frac{k_iR_AM}{k_{d_A} + (k_p + k_{fm})M + k_t(P + Q + S + 2T)} \tag{A.40}$$

$$S_1 = \frac{k_iR_BM}{k_{d_B} + (k_p + k_{fm})M + k_t(P + Q + S + 2T)} \tag{A.41}$$

$$T_1 = \frac{k_iR'M + k_{d_A}Q_1 + k_{d_B}S_1}{2[(k_p + k_{fm})M + k_t(P + Q + S + 2T)]} \tag{A.42}$$

E. Zeroth Moments of Live Polymers

Zeroth moments of live polymers are calculated by solving the following equations:

$$k_tP^2 + k_t(Q + S)P - A_0 = 0 \tag{A.43}$$

$$k_tQ^2 + [k_{d_A} + k_{fm}M + k_t(P + S)]Q - B_0 = 0 \tag{A.44}$$

$$k_tS^2 + [k_{d_B} + k_{fm}M + k_t(P + Q)]S - C_0 = 0 \tag{A.45}$$

$$k_tT^2 + [k_t(P + Q + S) + k_{fm}M]T - D_0 = 0 \tag{A.46}$$

where

$$A_0 = 2k_{dm}M^3 + k_{d_A}U + k_{d_B}V + (f_Rk_{d_A} + k_{fm}M)Q + (f_Rk_{d_B} + k_{fm}M)S + 4k_{fm}MT + k_iMR \tag{A.47}$$

$$B_0 = k_iR_AM + 2k_{d_A}U' + k_{d_B}W \tag{A.48}$$

$$C_0 = k_iR_BM + k_{d_A}W + 2k_{d_B}V' \tag{A.49}$$

$$D_0 = \tfrac{1}{2}[k_{d_A}Q + k_{d_B}S + 2k_iR'M] \tag{A.50}$$

F. First Moments of Live Polymers

$$\lambda_{P,1} = \frac{2(k_{fm}M + k_tP)\lambda_{T,1} + A_1}{k_{fm}M + k_t(P + Q + S)} \tag{A.51}$$

$$\lambda_{Q,1} = \frac{2k_tQ\lambda_{T,1} + B_1}{k_{d_A} + k_{fm}M + k_t(P + Q + S)} \tag{A.52}$$

$$\lambda_{S,1} = \frac{2k_tS\lambda_{T,1} + C_1}{k_{d_B} + k_{fm}M + k_t(P + Q + S)} \tag{A.53}$$

$$\lambda_{T,1} = \frac{D_{1_A}}{2D_{1_B}} \tag{A.54}$$

where

$$A_1 = 2k_{dm}M^3 + k_iRM + k_{d_A}\lambda_{U,1} + k_{d_B}\lambda_{V,1} + k_pMP + k_{fm}M(P + Q + S + 2T) \tag{A.55}$$

$$B_1 = k_iR_AM + 2k_{d_A}\lambda_{U',1} + k_{d_B}\lambda_{W,1} + k_pMQ \tag{A.56}$$

$$C_1 = k_iR_BM + k_{d_A}\lambda_{W,1} + 2k_{d_B}\lambda_{V',1} + k_pMS \tag{A.57}$$

$$D_{1_A} = 2k_iR'M + \frac{k_{d_A}B_1}{k_{d_A} + k_{fm}M + k_t(P + Q + S)} + \frac{k_{d_B}C_1}{k_{d_B} + k_{fm}M + k_t(P + Q + S)} + 2k_pMT \tag{A.58}$$

$$D_{1_B} = k_{fm}M + k_t(P + Q + S) - \frac{k_{d_A}k_tQ}{k_{d_A} + k_{fm}M + k_t(P + Q + S)} - \frac{k_{d_B}k_tS}{k_{d_B} + k_{fm}M + k_t(P + Q + S)} \tag{A.59}$$

G. Second Moments of Liver Polymers

$$\lambda_{P,2} = \frac{2(k_{fm}M + k_tP)\lambda_{T,2} + A_2}{k_{fm}M + k_t(P + Q + S)} \tag{A.60}$$

$$\lambda_{Q,2} = \frac{2k_tQ\lambda_{T,2} + B_2}{k_{d_A} + k_{fm}M + k_t(P + Q + S)} \tag{A.61}$$

$$\lambda_{S,2} = \frac{2k_tS\lambda_{T,2} + C_2}{k_{d_B} + k_{fm}M + k_t(P + Q + S)} \tag{A.62}$$

$$\lambda_{T,2} = \frac{D_{2_A}}{2D_{2_B}} \tag{A.63}$$

where

$$A_2 = 2k_{dm}M^3 + k_iRM + k_{d_A}\lambda_{U,2} + k_{d_B}\lambda_{V,2} + k_pM(2\lambda_{P,1} + P) + k_{fm}M(P + Q + S + 2T) + 4k_t\lambda_{P,1}\lambda_{T,1} \tag{A.64}$$

$$B_2 = k_i R_A M + 2k_{d_A}\lambda_{U',2} + k_{d_B}\lambda_{W,2} + k_p M(2\lambda_{Q,1} + Q) + 4k_t\lambda_{Q,1}\lambda_{T,1} \quad \text{(A.65)}$$

$$C_2 = k_i R_B M + k_{d_A}\lambda_{W,2} + 2k_{d_B}\lambda_{V',2} + k_p M(2\lambda_{S,1} + S) + 4k_t\lambda_{S,1}\lambda_{T,1} \quad \text{(A.66)}$$

$$D_{2_A} = 2k_i R'M + \frac{k_{d_A}B_2}{k_{d_A} + k_{fm}M + k_t(P + Q + S)} + \frac{k_{d_B}C_2}{k_{d_B} + k_{fm}M + k_t(P + Q + S)} + 2k_p M(2\lambda_{T,1} + T) + 4k_t\lambda_{T,1}^2 \quad \text{(A.67)}$$

$$D_{2_B} = k_{fm}M + k_t(P + Q + S) - \frac{k_{d_A}k_t Q}{k_{d_A} + k_{fm}M + k_t(P + Q + S)} - \frac{k_{d_B}k_t S}{k_{d_B} + k_{fm}M + k_t(P + Q + S)} \quad \text{(A.68)}$$

REFERENCES

1. K. Y. Choi and G. D. Lei, *AIChE J.*, **20,** 2067 (1987).
2. K. J. Kim and K. Y. Choi, *Chem. Eng. Sci.*, **44**(2), 197 (1988).
3. K. Y. Choi, W. R. Liang, and G. D. Lei, *J. Appl. Polym. Sci.*, **35,** 1547 (1988).
4. K. J. Kim, W. R. Liang, and K. Y. Choi, *Ind. Eng. Chem. Res.*, **28,** 131 (1989).
5. W. J. Yoon and K. Y. Choi, to appear.
6. Technical Bulletin, Pennwalt-Lucidol Company, 1986.
7. Q. W. Hui and A. E. Hamielec, *J. Appl. Polym. Sci.*, **16,** 749 (1972).
8. J. Brandrup and E. H. Immergut, *Polymer Handbook*, 3rd ed., Wiley, New York, 1990.
9. K. Arai, H. Yamaguchi, S. Saito, E. Sarschina, and T. Yamamoto, *J. Chem. Eng. Jpn.*, **19,** 413 (1986).
10. N. Friis and A. E. Hamielec, ACS Symp. Ser. 24, American Chemical Society, Washington, DC, 1976, p. 82.
11. A. I. Prisyazhnyuk and S. S. Ivanchev, *Polym. Sci. USSR*, **24,** 2051 (1970).
12. S. S. Ivanchev and Y. I. Zherebin, *Polym. Sci. USSR*, **16**(4), 956 (1974).

Received November 1, 1991
Accepted January 17, 1992